Optimized Fractional Order Based Droop Control with Improving the Flexibility of a Microgrid

Fatma-Zohra Hadjaidji[1,*], *Djamel* Boukhetala[1], and *Jean-Pierre* Barbot[2,3]

[1]Process Control Laboratory, Ecole Nationale Polytechnique 10 Avenue des Frères Oudek, BP 182, El Harrach, 16200, El Harrach Algiers, Algeria.
[2]Quartz Laboratory, ENSEA, 6, avenue du Ponceau 95014 Cergy-Pontoise Cedex France.
[3]LS2N UMR CNRS 6004 France.

Abstract. This work presents an improved four-levels hierarchical control strategy for flexible microgrid based on three-phase voltage source inverters (VSIs) connected in parallel. In the proposed strategy, zero-level control is required to handle current and voltage control of VSIs. The primary-level that consists of a decentralized controller is based on a modified universal droop control by introducing a fractional-order derivative. It is used to enhance the power sharing quality during islanded mode and the desired power generation in grid-connected mode. In the secondary centralized control, the voltage and frequency deviations caused by the primary-control are restored. Also, this level includes the synchronization control loop that enables a seamless transition between both operation modes. In order to improve the flexibility of the microgrid, a sequential logic approach is proposed in the tertiary level. It is exploited to manage both the restoration and the synchronization loops at each transition, as well as the static switch (SS) which is used to connect/disconnect the microgrid to/from the main grid. The control parameters are optimized by using the self-learning particle swarm optimizer (SLPSO) algorithm. Simulations were performed to highlight the performances of the proposed hierarchical control approach compared with the well-known three-levels control scheme.

1 Introduction

In recent years, the world has witnessed high levels of atmospheric pollution through large emissions of toxic gases that is a consequence of the high demand primarily for electric power [1], which gave an incentive to exploit renewable energy sources (RES)s such as wind energy, photovoltaic, tidal energy, thermal energy, etc, as clean and inexhaustible power sources to enhance energy security of countries and reduce imports of fossil fuels that are polluting the environment [2]. The RESs has gone through many stages of technological development in order to use them as an alternative to traditional energy sources in modern power grids and to facilitate support for the electrification of isolated

* Fatma-Zohra Hadjaidji: fatma_zahra.hadjaidji@g.enp.edu.dz

rural communities as well as affordability. The use of RESs also allows a transition from centralized production (the traditional model) to decentralized energy production.

The microgrid presents a privileged approach for the integration of decentralized energy resources. It combines multiple local production and distribution installations composed of distributed generation (DG) units, storage systems and loads. The considered DGs integrated with the AC microgrids are based on VSIs connected with passive harmonic filters to produce a scheduled voltage with a synchronous frequency. They are connected in parallel to the same bus with a local linear or nonlinear load. The microgrid can operate autonomously by handling power quality issues as well as interact with the main grid or with other microgrids, thus creating a Smart Grid. The microgrid is connected with the main grid via SS.

In this context, a new robust controller called the universal droop control is developed in [3], for an accurate power sharing regardless of the output impedance of the VSIs when the microgrid operates in islanded mode. Recent research is directed to design a hierarchical control for flexible operation of a microgrid [4]. The structure of this control strategy consists of three levels; inner, primary and secondary. The inner control is based on a cascade proportional resonant controller to get a better voltage and current regulation with less harmonics. A developed droop control is proposed as a primary controller. It makes the universal droop control able to handle the grid-connected mode. The secondary controller is required to restore the amplitude and frequency deviations caused by the primary controller. Also, it synchronizes the microgrid voltage with the main grid voltage for a smooth transition. Both the restoration loop and the synchronization loop and SS are not methodically managed at each transition.

In this work, a fractional order derivative is introduced to the universal droop control proposed in [4]. A tertiary level control, based on a sequential logic approach, is added to increase the flexibility of the microgrid. This level allows the secondary controller loops to operate autonomously, as well as the SS. The dynamic performances of the developed four levels hierarchical control are highlighted via simulations using MATLAB/SIMULINK, for a microgrid with three VSIs connected in parallel and a local nonlinear load.

The remainder of this paper is organized as follows: Section 2 presents the overall structure of the proposed four levels hierarchical control scheme. The improved primary control level with fractional order derivative including the inner controller is described. The PI centralized controller of the secondary level is presented. A sequential logical management strategy is developed for the tertiary control level. Optimized control parameters via SLPSO algorithm are given in section 3. Section 4 illustrates comparative simulation results with the well-known three levels control scheme. Section 5 concludes the paper.

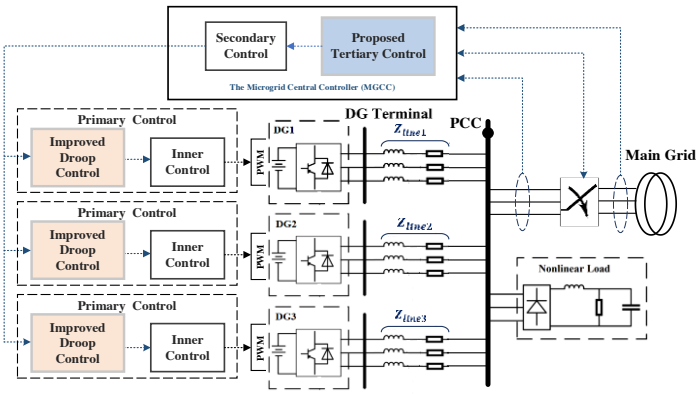

Fig. 1. Block diagram of the microgrid including proposed hierarchical control scheme.

2 Proposed hierarchical control scheme

In the case of flexible microgrid based on three phase VSIs operated in parallel, a four levels hierarchical control is proposed to supply nonlinear local loads through LCL filter and a line impedance representing the physical distance (see Fig.1). Moreover, it is developed to ensure a smooth transition between the islanded and the connected mode.

2.1 Improved primary control

Modern control techniques allow improving the control systems performances and robustness such as the fractional order control [5]. In this work, the primary controller presented in [4] is replaced by a fractional order one in order to enhance performances of the power sharing at each transition, load variations, plug and play operation as well as the transition between different operating modes.

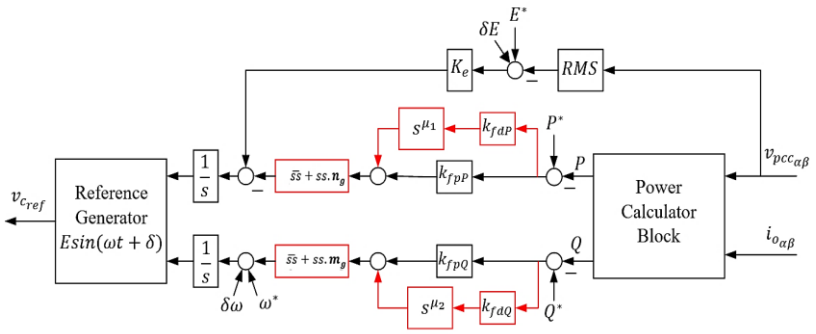

Fig. 2. Schematic diagram of the improved droop control.

The new droop controller is expressed as follow:

$$\dot{E} = K_e\left(E^* - V_{pcc}\right) - \left(k_{fpP}(P-P^*) + \boldsymbol{k_{fdP}D_t^{\mu_1}(P-P^*)}\right)\left(\bar{ss} + ss.\boldsymbol{n_g}\right) \quad (1)$$

$$\omega = \omega^* + \left(k_{fpQ}(Q-Q^*) + \boldsymbol{k_{fdQ}D_t^{\mu_2}(Q-Q^*)}\right)\left(\bar{ss} + ss.\boldsymbol{m_g}\right) \quad (2)$$

E and ω are the voltage magnitude and the frequency of the capacitor voltage. E^* and ω^* are their nominals. V_{pcc} is the voltage magnitude (RMS) of common coupling (PCC) voltage. $P^*$and Q^* are the imposed active and reactive power during the connected grid mode.

K_e is a universal droop control gain. k_{fpP} and k_{fpQ} are the static droop coefficients given that are calculated by using the desired voltage ratio $e_P = \frac{k_{fpP}S^*}{K_eE^*}$ and frequency boost ratio $e_Q = \frac{k_{fpQ}S^*}{\omega^*}$; Where e_P= 0.1, e_Q=0.001 as given in [4]. S^* is the desired apparent power.

k_{fdP} and k_{fdQ} are fractional derivative droop gains of real and reactive power, respectively. n_g and m_g are the hybrid droop coefficient and ss is a hybrid variable where:

$$ss = \begin{cases} 0 & \text{Microgrid operates in off} - \text{grid mode} \\ 1 & \text{Microgrid operates in on} - \text{grid mode} \end{cases} \quad (3)$$

$D_t^{\mu_i}$ is the non-integer μ_i^{th} order derivation operator $\left(\frac{d}{dt}\right)^{\mu_i}$ with $\{\mu_{1,2} \in \mathcal{R}^+ / \ 0 < \mu_1, \mu_2 < 2\}$. Therefore, Laplace representation of the fractional-order operator is presented according to Grünwald-Letnikov in [5] as follow:

$$L\left(k_{fdP}\boldsymbol{D_t^{\mu_1}}(P(t)-P^*)\right) = k_{fdP}\boldsymbol{s^{\mu_1}}(P(s)-P^*) \quad (4)$$

$$L\left(k_{fdQ}\boldsymbol{D_t^{\mu_2}}(Q(t)-Q^*)\right) = k_{fdQ}\boldsymbol{s^{\mu_2}}(Q(s)-Q^*) \quad (5)$$

The method proposed by Oustaloup in [6] is based on the fractional order approximation by a function of a recursive filter called the Oustaloup filter. Considering $[\omega_b, \omega_h]$ as the frequency band, The Oustaloup recursive approximation of $\boldsymbol{s^{\mu_i}}$ operator shown in Fig.2 is expressed by the following transfer function:

$$\hat{G}(s) = K.\prod_{k=-N}^{N}\frac{(s+\omega_k')}{(s+\omega_k)} \quad (6)$$

Where:

$$\begin{aligned} K &= \omega_h^{\boldsymbol{\mu_i}} \\ \omega_k' &= \omega_b\left({}^{\omega_h}/_{\omega_b}\right)^{\left(\frac{k+N+0.5(1-\boldsymbol{\mu_i})}{2N+1}\right)} \\ \omega_k &= \omega_b\left({}^{\omega_h}/_{\omega_b}\right)^{\left(\frac{k+N+0.5(1+\boldsymbol{\mu_i})}{2N+1}\right)} \end{aligned} \quad (7)$$

$(2N+1)$ is the filter order.
P and Q in Fig.2 are the active and the reactive power delivered by the power inverter. They are calculated from v_{pcc} and i_o through the following expression [7]:

$$p = v_{pcc_\alpha} i_{o_\alpha} + v_{pcc_\beta} i_{o_\beta} \quad (8)$$

$$q = v_{pcc_\beta} i_{o_\alpha} - v_{pcc_\alpha} i_{o_\beta} \quad (9)$$

p and q are the instantaneous active and reactive power, $v_{pcc_{\alpha\beta}}$ and $i_{o_{\alpha\beta}}$ are the PCC voltage and the output current given by using the $\alpha\beta$ transformation. Low pass filters are applied to obtain P and Q (Power Calculator Block).

The signal generated by the droop control through power sharing is considered as a reference signal $v_{c_{ref}}$ of the capacitor voltage controller.

The zero level called the inner control is dedicated to cascading voltage and current control of VSI via the capacitor voltage and inductance current respectively as depicted in Fig 3. The proportional resonant (PR) controllers are adopted for both control loops. The transfer function of the PR controller is given as:

$$G_{PR}(s) = k_p + \frac{k_r s}{s^2 + \omega_c s + {\omega_0}^2} + \sum_{h=3,5,7}\frac{k_h s}{s^2 + h\omega_c s + (h\omega_0)^2} \quad (10)$$

where k_p is the proportional gain, k_h is the resonant gains at the h-harmonic, ω_0 and ω_c represent the fundamental frequency and the resonance bandwidth.

This control is accomplished by using Clarke transformation to convert three phase system (abc) into two independent single-phase system $(\alpha\beta)$, (see [4]).

An optimization algorithm is used to obtain the primary control parameters as well as the inner control ones.

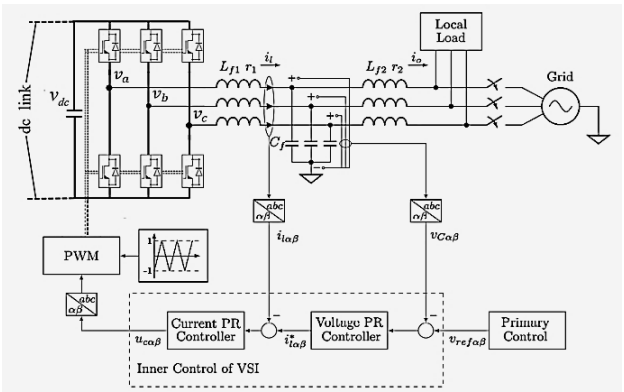

Fig. 3. Schematic diagram of the zero-level control of the DG.

2.2 Secondary centralized control

The frequency and voltage magnitude deviations from their rated values that occur at the PCC are a consequence of the droop control characteristics. The secondary control is required to compensate these deviations. The expressions of both restoration compensators based on the PI-type controller are expressed as follow.

$$\delta\omega_{res} = k_{p\omega}\left(\omega^*_{pcc} - \omega_{pcc}\right) + k_{i\omega}\int\left(\omega^*_{pcc} - \omega_{pcc}\right)dt \qquad (11)$$

$$\delta E_{res} = k_{pE}\left(E^*_{pcc} - V_{pcc}\right) + k_{iE}\int\left(E^*_{pcc} - V_{pcc}\right)dt \qquad (12)$$

where $k_{p\omega}$, k_{pE} are the proportional restoration controllers parameters, $k_{i\omega}$ and k_{iE} are their integral ones. ω_{pcc} is the frequency of common coupling (PCC) voltage.

Moreover, a third control loop is included within the secondary control scope when the grid connection mode is expected. It synchronizes the microgrid with the main grid for a smooth transition by reducing the phase shift between their voltages. Then, an amount of frequency ω_s is sent to each VSI primary control through the secondary control.

The synchronization controller is given by using $\alpha\beta$ components variables of the PCC and the grid voltages. For this end, the following equation must be satisfied:

$$\langle v_{pcc_\alpha} v_{g_\beta} - v_{pcc_\beta} v_{g_\alpha} \rangle = 0 \qquad (13)$$

PI controller G_{syn} dedicated for synchronization control loop can be integrated as:

$$\omega_s = \left(v_{pcc_\alpha} v_{g_\beta} - v_{pcc_\beta} v_{g_\alpha}\right) G_{LPF}(s) G_{syn}(s) \qquad (14)$$

Where

$$G_{syn}(s) = \frac{k_p s + k_i}{s} \qquad (15)$$

$$G_{LPF}(s) = \frac{\omega_{LPF}}{\omega_{LPF} + s} \qquad (16)$$

k_p and k_i are the PI coefficients, ω_s is the output of the synchronization loop.
G_{LPF} is a low-pass filter which is used for low bandwidth communications to all VSIs operate in parallel, ω_{LPF} is its frequency and is selected as $\omega_0/10$.

2.3 The proposed tertiary level

The Microgrid concept has been proposed for flexible and efficient utilization of DGs. Then, with the increasing penetration of distributed generation, the modern control and management techniques are becoming increasingly attractive, as they offer higher flexibility and lower implementation cost [8]. This section deals with the development of a management framework dedicated to the tertiary level in order to make the secondary controller loops operate autonomously, as well as the switch (SS). We present a simple sequential logic approach that can be easily implemented. The operating principle of this approach is the combination of the sequential binary logic outputs: SC, SYN and ss which are used to On/Off the restoration loop, the synchronization control and the SS switching, respectively.

Let consider that e is the error between the PCC rated and the reference voltage $\left(e = V_{ref} - V_{pcc}\right)$, δe is its variation ($\delta e = de/dt$) and k a time instant.

It is known that to ensure the global system stability, the primary control dynamic must be faster than the secondary control one. The secondary control is responsible for eliminating any steady state error e caused by the droop control. Indeed, the restoration loop is activated only when the tracking error becomes a non-null constant and its variation takes a very small value. However, this loop is deactivated just in the case when tracking error converges. The synchronization process can work only when the restoration loop is out of order. That is what ensure higher power quality compared with [4] during the transition from islanded to grid-connected mode. For these purposes, the following strategy is proposed in a tertiary level.

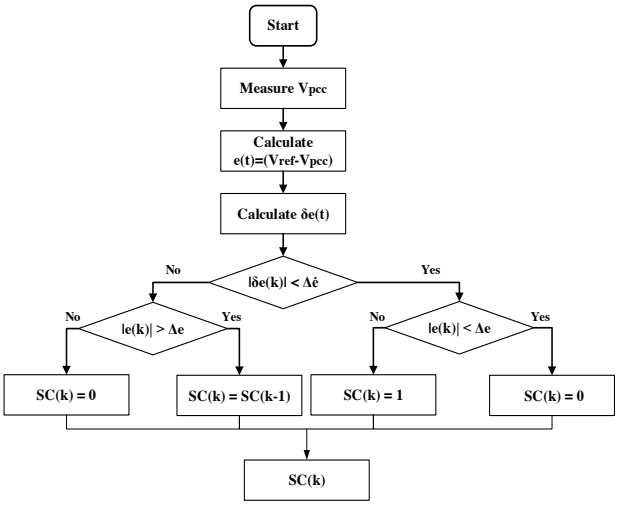

Fig. 4. Flow chart for SC signal in the proposed tertiary control strategy.

The decision variables in the time instant k are expressed as follow, respectively for On/Off of the restoration loop, the synchronization control and the SS switching.

$$SC(k) = \begin{cases} SC(k-1) & if \quad |\delta e(k)| > \Delta \dot{e} \; \boldsymbol{AND} \; |e(k)| > \Delta e \\ 1 & if \quad |e(k)| > \Delta e \\ 0 & if \quad else \end{cases} \tag{17}$$

$$SYN(k) = \begin{cases} 1 & if \quad g_c = 1 \; \boldsymbol{AND} \; SC = 0 \\ 0 & if \quad g_c = 0 \; \boldsymbol{AND} \; SC = 1 \\ SYN(k-1) & if \quad else \end{cases} \tag{18}$$

$$ss(k) = \overline{SC} * \bar{\Phi} * g_c \text{ ; Where } \Phi = \begin{cases} 0 & if \quad |\varphi| < \Delta\varphi \\ 1 & if \quad else \end{cases} \tag{19}$$

φ is the phase difference between the PCC voltage and the grid voltage. g_c is binary signal expressing the intention of grid-disconnection ($g_c = 0$) or grid-connection ($g_c = 1$). Δe , $\Delta\dot{e}$ and $\Delta\varphi$ are very small values of e, δe and φ, respectively and * is the logical product operator.

The proposed tertiary level strategy algorithm for the restoration loop is illustrated through the flow chart shown in Fig. 4.

3 Optimal control parameters-tuning

Optimal parameters of the hierarchical control are calculated by using the metaheuristic so called Self learning particle swarm optimizer (SLPSO) algorithm [9], which is based on the minimization of a fitness function.

The SLPSO is an improved optimization structure of the classical PSO through learning techniques that are introduced for each particle k by using the following four operators, respectively:

- Operator 1: learning from its individual best particle (p_{best}) position

$$Exploitation : \mathbf{v_k^d} = \omega\mathbf{v_k^d} + \eta\mathbf{r_k^d}\left(\mathbf{pbest_k^d} - \mathbf{x_k^d}\right) \tag{20}$$

- Operator 2: learning from a random position nearby

$$Jumping\ out: \mathbf{x_k^d} = \mathbf{x_k^d} + \mathbf{v_{avg}^d}.N(0,1) \tag{21}$$

- Operator 3: learning from the p_{best} of a random particle

$$Exploration : \mathbf{v_k^d} = \omega\mathbf{v_k^d} + \eta\mathbf{r_k^d}\left(\mathbf{pbest_{k_{nearest}}^d} - \mathbf{x_k^d}\right) \tag{22}$$

- Operator 4: learning from the global best particle archive (a_{best}) position

$$Convergence : \mathbf{v_k^d} = \omega\mathbf{v_k^d} + \eta\mathbf{r_k^d}\left(\mathbf{abest^d} - \mathbf{x_k^d}\right) \tag{23}$$

The PR parameters vector of the inner control is given by:

$$\boldsymbol{\theta} = \left[\omega_c, k_{pv}, k_{rv}, , k_{3v}, k_{5v}, k_{7v}, k_{pi}, k_{ri}, , k_{3i}, k_{5i}, k_{7i}\right]^T$$

The proposed fitness function is expressed as follow:

$$F_{PR}(\boldsymbol{\theta}) = \sum_{t=0}^{\infty}\left(\left(v_{ref_a}^t - v_{c_a}^t(\boldsymbol{\theta})\right)^2 + \left(v_{ref_b}^t - v_{c_b}^t(\boldsymbol{\theta})\right)^2 + \left(v_{ref_c}^t - v_{c_c}^t(\boldsymbol{\theta})\right)^2\right) \tag{24}$$

In order to increase the performance of the proposed droop control and secondary control, another fitness function is defined, to optimize all of their control parameters, as [4]:

$$F(\boldsymbol{\theta}) = \sum_{t=0}^{\infty} t|e_t(\boldsymbol{\theta})|\left[1 + \lambda - \lambda sign\left(e_t(\boldsymbol{\theta})\right)\right] \tag{25}$$

Being $e_t(\boldsymbol{\theta})$ the difference between setpoint and real value by using θ and λ is a constant coefficient that penalizes the oscillations.

In islanded mode, $\boldsymbol{\theta_1^1} = \left[K_e, \boldsymbol{k_{dP}}, \boldsymbol{k_{dQ}}\right]^T$ is the parameters vector of the classical droop control and $\boldsymbol{\theta_1^2} = \left[K_e, \boldsymbol{k_{fdP}}, \boldsymbol{k_{fdQ}}, \boldsymbol{\mu_1}, \boldsymbol{\mu_2}\right]^T$ is the parameters vector of the proposed droop control. In grid connected mode, both droop controls need the optimal of $\boldsymbol{\theta_2} = \left[n_g, m_g\right]^T$. The PI controller parameters vector of each secondary control loop is given by $\boldsymbol{\theta} = \left[k_p, k_i\right]^T$ The optimal parameters of the global control of the system presented in section 4 are shown in Table 1, with λ = 50, Δe=0.2V,$\Delta \dot{e}$=4V/s, $N = 2$ (Oustaloup filter order). and $[\omega_b, \omega_h] = [10^{-2}, 10^3]$.

Table 1. Hierarchical control system parameters.

Inner control

	$\boldsymbol{\omega_c}$	$\boldsymbol{k_p}$	$\boldsymbol{k_r}$	$\boldsymbol{k_3}$	$\boldsymbol{k_5}$	$\boldsymbol{k_7}$
$\boldsymbol{G_{PR_v}}$	0.0016	0.25	200.94	26.3	22.56	67.11
$\boldsymbol{G_{PR_i}}$	0.0016	0.1925	221.02	40.29	98.17	61.04

Classical droop control ($\boldsymbol{\mu_1 = \mu_2 = 1}$)

	$\boldsymbol{K_e}$	$\boldsymbol{k_{pP}}$	$\boldsymbol{k_{pQ}}$	$\boldsymbol{k_{dP}}$	$\boldsymbol{k_{dQ}}$	$\boldsymbol{n_g}$	$\boldsymbol{m_g}$
$\boldsymbol{VSI_1}$	11.6	0.2890	2.5×10^{-4}	0.0019	2.8×10^{-6}	0.03	5.1
$\boldsymbol{VSI_2}$	11.6	0.1089	1.6×10^{-4}	0.0039	3.3×10^{-6}	0.03	5.1
$\boldsymbol{VSI_3}$	11.6	0.0871	1.3×10^{-4}	0.0046	1.7×10^{-6}	0.03	5.1

Fractional order droop control

	$\boldsymbol{K_e}$	$\boldsymbol{k_{fpP}}$	$\boldsymbol{k_{fpQ}}$	$\boldsymbol{k_{fdP}}$	$\boldsymbol{k_{fdQ}}$	$\boldsymbol{\mu_1}$	$\boldsymbol{\mu_2}$
$\boldsymbol{VSI_1}$	13	0.3222	2.5×10^{-4}	0.0025	7.18×10^{-7}	1.135	1.35
$\boldsymbol{VSI_2}$	13	0.2014	1.6×10^{-4}	0.0014	9.05×10^{-6}	1.154	0.88
$\boldsymbol{VSI_3}$	13	0.1611	1.3×10^{-4}	0.0038	7.89×10^{-6}	0.961	0.97

Secondary control

	Voltage loop	**Frequency loop**	**Synchronization**
$\boldsymbol{k_p}$	1.8815	2.2586	3.8
$\boldsymbol{k_i}$	4.2972	7.708	0

4 Simulation Results

In order to test the feasibility of the proposed four levels hierarchical control, simulations are performed by using FOMCON Toolbox [10], a simulation Microgrid setup was built as depicted in Fig. 1, with the hierarchical control system and physical parameters given in Table 1 and Table 2, respectively.

Table 2. Physical parameters.

Electrical system parameters

parameters	**Symbol**	**Value**	**Unit**
Rated voltage	E^*	220	V
Nominal frequency	ω^*	2π50	rad/s
Load inductance	L_l	84	μH
Load capacitance	C_l	500	μC
Load	R_l	100/140/145/60/150	Ω

VSIs parameters

DC voltage	V_{dc}	650	V
Filter inductor	$L_{lf1,2}; r_{l1,2}$	1.8; 0.03	$mH;\ \Omega$
Filter capacitor	$C_{lf1,2}$	35	μC
PWM frequency	f_s	10	kHz
Output impedance	Z_o	Z_{o1}: 2.8; 0.7 Z_{o2}: 1.7; 0.5 Z_{o3}: 1,6; 0.8	$mH;\ \Omega$
Apparent power rating	S	1250/2000/2500	kVA

The test microgrid consists of three parallel DG units each one is composed of VSI and LCL filter, and a nonlinear load, connected between them through line impedance Z.

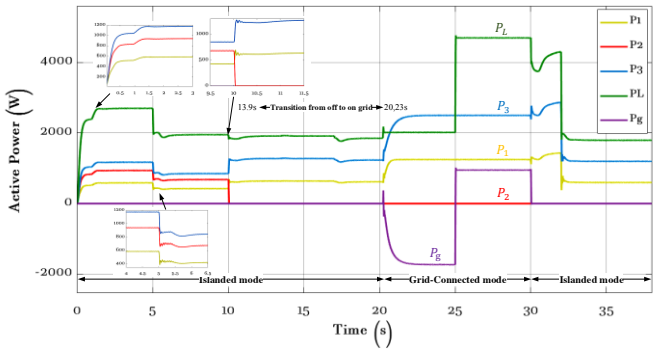

(a)

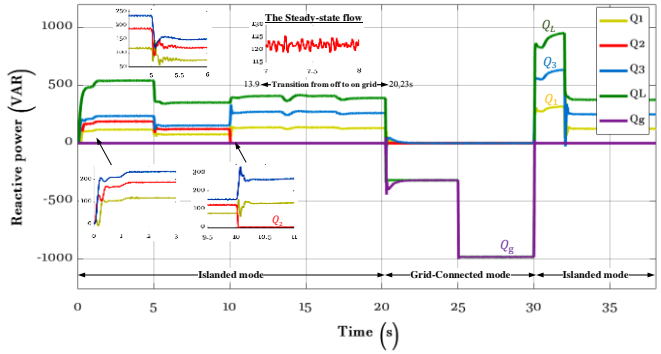

(b)

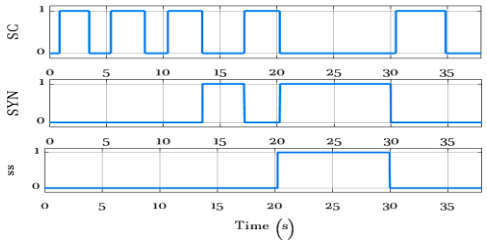

(c)

Fig. 5. Simulation results of Primary control and Tertiary level strategy scheme using the classical Droop Control (a) Active power; (b) Reactive power; (c) {SC; SYN; ss}.

In order to validate the improved droop control presented in this work, as well as the tertiary level strategy, different scenarios are simulated. After the operation start of the microgrid, the load demand is increased at t=5s which requires more power supply from the three connected DGs. The disconnection of the second DG (VSI2), at t=10s is also simulated. For a smooth transition from islanded mode to grid connected mode, the binary signal gc is transmitted to the tertiary control at t=12s to activate the synchronization process in order to eliminate the phase error between the PCC and main grid voltages. However, by according the strategy proposed in tertiary level, the synchronization process only works when the PCC voltage is restored, at t=13.9s by using the classical droop control and at t=13.4s by using the order-fractional one, as shown in Fig.5. and Fig.6.

In Fig.5. it is shown that by using the classical droop control, another load variation test is simulated at t=17s, which makes the synchronization loop out of order, to complete the restoration of the PCC voltage. While, the non-integer order droop control, thanks to its rapidity compared with the classical one, allows the microgrid to connect to the main grid before load variation at t=16.95s (see Fig.5 and Fig.6).

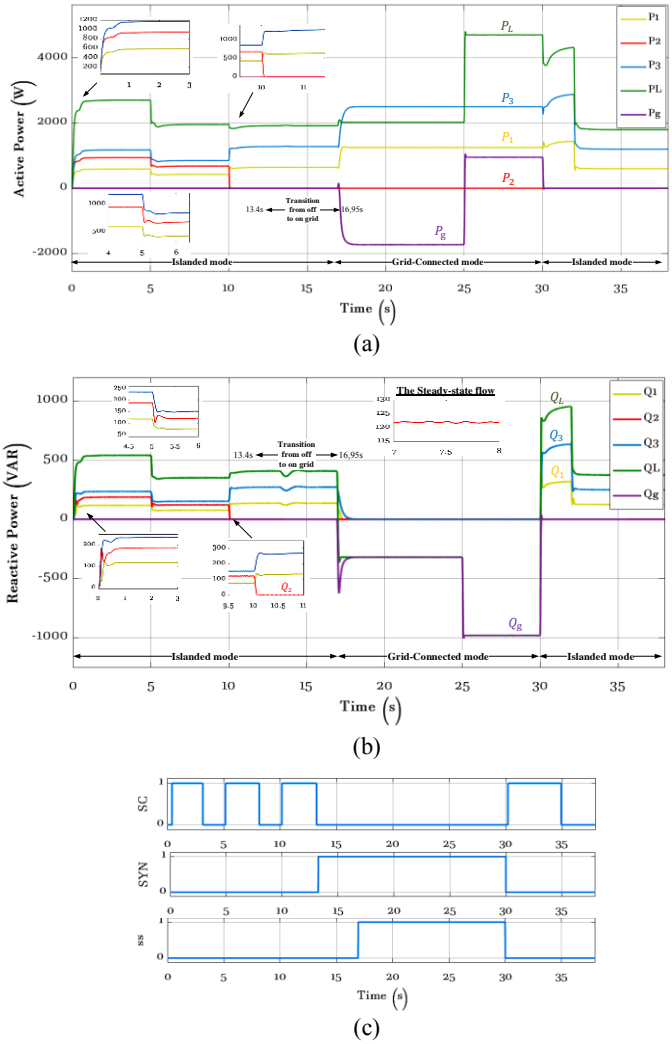

(a)

(b)

(c)

Fig. 6. Simulation results of Primary control and Tertiary level strategy scheme using the Fractional-Order Droop Control (a) Active power; (b) Reactive power; (c) {SC; SYN; ss}.

According to Fig.5, Fig.6 and Fig.7, the simulation results demonstrate that, during each transient state, the proposed primary control with a fractional order derivative performs better than the one with the integer order in terms of a time response, overshoot and oscillations during steady-state flow, namely for the reactive power.

The performance of the binary sequential management strategy proposed for the tertiary level is illustrated via Fig.5(c) and Fig.6(c). This strategy proves its efficiency to make the secondary controller loops work autonomously, as well as the switch (SS). The restoration controller is started only when the droop control outputs are in steady state. Also, for a smooth transition to the connected-grid mode, the synchronization loop doesn't work until the restoration process is not completed. The switch SS is activated once the PCC and the main grid voltages are synchronized as shown in Fig.7. (d).

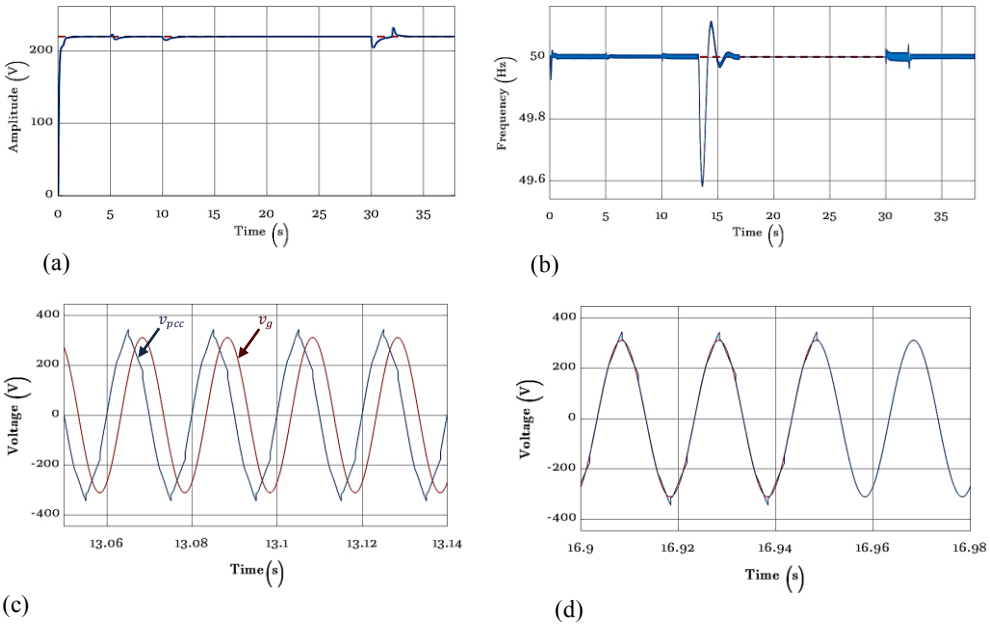

Fig. 7. Simulation results of Secondary control using the Fractional-Order Droop Control (a) PCC voltage amplitude; (b) Frequency; (c) and (d) The synchronization process between PCC and main grid voltage

5 Conclusion

In this paper, a four levels hierarchical control structure with a fractional order droop control is proposed for a three DGs flexible microgrid. The first level control which is called the primary control is based on an improved universal droop control developed in [4] by introducing a fractional order derivative operator. The output signal of the primary controller serves as a reference voltage for the inner controller (zero level) which is dedicated to cascading voltage and current control of VSI via the capacitor voltage and inductance current, respectively. In the secondary control, the magnitude and the frequency restorations loops are presented to compensate the deviations caused by the droop control loop. Also, this level includes the synchronization control loop. Most of control parameters are calculated by using the self-learning particle swarm optimizer (SLPSO) algorithm. A tertiary level is added in order to ensure higher flexibility of the microgrid and the power quality during transition mode. In this last level, a sequential logical strategy is proposed to ensure smooth

transition between different modes of operation. Simulations are performed to highlight the performances of the proposed control scheme compared with the known three level hierarchical one.

This work was supported by the DGRSDT of the Ministry of Higher Education and Scientific Research of Algeria, Quartz Laboratory, ENSEA, France and LS2N UMR CNRS 6004 France.

References

1. IEA (2021), Global Energy Review 2021, https://www.iea.org/reports/global-energy-review-2021, IEA, Paris (April 2021)
2. A. Llaria, O. Curea, J. Jiménez, and H. Camblong, Survey on microgrids: Unplanned islanding and related inverter control techniques, Renewable Energy, vol. **36**, pp. 2052-2061 (8//2011)
3. Q. C. Zhong and Y. Zeng, Universal droop control of inverters with different types of output impedance, IEEE Access, vol. **4**, pp. 702–712 (2016)
4. I. Ziouani, D. Boukhetala, A-M. Darcherif, B. Amghar, and I. EL Abbassi, Hierarchical control for flexible microgrid based on three-phase voltage source inverters operated in parallel, Int. J. Electrical Power & Energy Systems, 95C, pp. 188-201 (2018)
5. N. Bouarroudj, Fractional order sliding mode control optimized by metaheuristics: application to nonlinear and interconnected systems, PhD thesis, ENP Algiers (2017)
6. A. Oustaloup, F. Levron, B. Mathieu, and F. M. Nanot, Frequency-Band Complex Noninteger Differentiator: Characterization and Synthesis, IEEE transactions on circuits and systems-I: fundamental theory and applications, vol. **47**, nO 1, pp. 25-39 (January 2000)
7. E. Hoff and T. Skjellnes, paralleled three-phase inverters, NORPIE'2004 Conf., pp. 1 – 6, in Proc (2004)
8. A. Elmouatamid, R. Ouladsine, M. Bakhouya, N. El Kamoun, M. Khaidar, K. Zine-Dine, Review of Control and Energy Management Approaches in Micro-Grid Systems. Energies 2021, **14**, 168 (2021)
9. C. Li, S. Yang, T. T. Nguyen, A self-learning particle swarm optimizer for global optimization problems, IEEE Transactions on Systems, Man, and 435 Cybernetics, Part B (Cybernetics) **42** (3) (2012)
10. A. Tepljakov, E. Petlenkov and J. Belikov, FOMCON: Fractional-order modeling and control toolbox for MATLAB, in Proceedings of the 18th International Conference Mixed Design of Integrated Circuits and Systems - MIXDES 2011, Gliwice (2011)